

# PROCEEDINGS

## AMERICAN SOCIETY OF CIVIL ENGINEERS

JULY, 1955



### MINIMUM PRESSURES IN RECTANGULAR BENDS

by M. B. McPherson, A.M. ASCE,  
and H. S. Strausser, J.M. ASCE

HYDRAULICS DIVISION

*{Discussion open until November 1, 1955}*

Copyright 1955 by the AMERICAN SOCIETY OF CIVIL ENGINEERS  
Printed in the United States of America

**Headquarters of the Society**  
33 W. 39th St.  
New York 18, N. Y.

PRICE \$0.50 PER COPY

## THIS PAPER

--represents an effort by the Society to deliver technical data direct from the author to the reader with the greatest possible speed. To this end, it has had none of the usual editing required in more formal publication procedures.

Readers are invited to submit discussion applying to current papers. For this paper the final date on which a discussion should reach the Manager of Technical Publications appears on the front cover.

Those who are planning papers or discussions for "Proceedings" will expedite Division and Committee action measurably by first studying "Publication Procedure for Technical Papers" (Proceedings Paper No. 290). For free copies of this Paper—describing style, content, and format—address the Manager, Technical Publications, ASCE.

Reprints from this publication may be made on condition that the full title of paper, name of author, page reference, and date of publication by the Society are given.

The Society is not responsible for any statement made or opinion expressed in its publications.

This paper was published at 1745 S. State Street, Ann Arbor, Mich., by the American Society of Civil Engineers. Editorial and General Offices are at 33 West Thirty-ninth Street, New York 18, N. Y.

## MINIMUM PRESSURES IN RECTANGULAR BENDS

M. B. McPherson,<sup>1</sup> A.M. ASCE

and

H. S. Strausser,<sup>2</sup> J.M. ASCE

### INTRODUCTION

The accurate prediction of minimum pressures which occur in bends has been a source of confusion for some time. It is no longer questionable that these minimum pressures can, under the proper conditions, become low enough to cause cavitation. The purpose of this paper is to suggest a basis for predetermining the magnitude of pressures associated with cavitation in a bend of rectangular cross-section. The authors have in mind the design of large bends which are frequently part of dam outlet structures, siphons and other large conduit bends, particularly those with limited or small "back pressures."

The mechanics of flow through bends have been explained quite thoroughly; however, practical methods for the realistic application of this mechanics have been only sparsely advanced. This paper is a modified digest of one phase of an unpublished thesis,<sup>(1)3</sup> which included a study of circular bends; the material on circular bends has recently been expanded.<sup>(2)</sup>

Various observers have proposed the idea that in closed bends, the velocity distribution should be and is near-potential with  $vn = a$  constant. The reader is referred to Figure 1 for definitions of terms used herein. Pfarr<sup>(3)</sup> was the first to suggest that the centerline of the bend and the center streamline, along which the tangential velocity is equal to the average velocity, are not coincident for potential flow. With potential flow  $vn = K = v_1 r_1 = v_0 r_0$  and

$$dQ = v b \, dn; \quad Q = \int_{r_1}^{r_0} b \frac{K}{n} \, dn = b K \ln \frac{r_0}{r_1}.$$

For the radius,  $r_m$ , where one would expect to find the average velocity,  $V$ ,  $K = V r_m$  and

$$r_m = \frac{r_0 - r_1}{\ln r_0 / r_1} = \frac{2c}{\ln r_0 / r_1} \quad . \quad . \quad . \quad (1)$$

Experimental confirmation of these ideas was first carried on by Lell<sup>(4)</sup> and later tests on closed spillway models by Shukry,<sup>(5)</sup> Davies and Puranik<sup>(6)</sup> and

1. Associate Prof. of Civ. Eng., Lehigh Univ., Bethlehem, Pa.

2. Asst. Prof. of Mechanics, Lehigh Univ., Bethlehem, Pa.

3. Numerals in parentheses thus: (1), refer to corresponding items in the list of references (see appendix).

Gibson, Asprey and Tattersall,<sup>(7)</sup> for example, indicated pressure and/or velocity distributions approximating those for potential or irrotational motion. (Practically all model studies reported have been performed on rectangular bends.)

#### Position and Correlation of Maximum ( $h_0 - h_1$ )

From available evidence, the proper location of taps for the determination of maximum ( $h_0 - h_1$ ) should be at the mid-height ( $b/2$ ) of the side walls. For example, in Leil's experiments, 5 taps were evenly spaced from top to bottom of the inside and outside walls. His measurements showed the maximum and minimum piezometric head to be at mid-height. This is consistent with the concept of secondary motion in a bend.

Present data from Leil, Yarnell and Woodward,<sup>(8)</sup> Silberman<sup>(9)</sup> and two model studies at Lehigh University indicate that the maximum piezometric differential occurs at or near the  $45^\circ$  cross-section for  $90^\circ$  &  $180^\circ$  bends. This is not to infer that the maximum ( $h_0 - h_1$ ) is necessarily found at the same cross-section as the minimum piezometric head at the inside of the bend. However, the points where the maximum ( $h_0 - h_1$ ) and the minimum piezometric head occur are not far apart spatially.

A useful term suggested by Lansford<sup>(10)</sup> is the "Bend Coefficient,"  $C_k$ , defined as  $\frac{(h_0 - h_1)}{v^2/2g}$ . In potential (frictionless) flow,  $K = V r_m = v_i r_i = v_o r_o$  and  $h_1 + v_1^2/2g = h_0 + v_o^2/2g = h_m + V^2/2g$ . Combining these terms with Equation (1) yields

$$C_k = \frac{\left(\frac{K}{r_1}\right)^2 - \left(\frac{K}{r_o}\right)^2}{\frac{K^2 (\ln r_o/r_1)^2}{4c^2}}$$

and if  $x = R/c$ ,

$$C_k = \frac{\frac{4}{(x-1)^2} - \frac{4}{(x+1)^2}}{\left(\ln \frac{x+1}{x-1}\right)^2}$$

which can also be expressed as

$$C_k = \frac{16x}{\left(\ln \frac{x+1}{x-1}\right)^2 (x^2-1)^2} \quad \cdot \quad \cdot \quad \cdot \quad (2)$$

To show that the maximum value of ( $h_0 - h_1$ ) for actual flow is related to the piezometric head distribution for potential motion, a plot of  $C_k$ (data) versus  $x = R/c$  is shown in Fig. 2., as well as a plot of Equation (2). The ( $h_0 - h_1$ ) selected from the data for use in this plot is that occurring at  $45^\circ$ , regardless of the value of  $\theta$ , since this differential included, in general, the

maximum value of  $(h_0 - h_1)$  as well as the smallest value of  $h_1$ . In the case of Lell's data, where 45° taps were lacking, the value shown was obtained from plots of comprehensive head distribution data.

A similar plot taken from data by Nippert<sup>(11)</sup> is shown separately in Fig. 3. Because of the small internal dimensions of his bends (8 mm. to 60 mm.), plus the fact that the test bends were preceded almost immediately by a gradual contraction, eccentric to the bend, very close agreement with the theoretical cannot be expected. It is presented here for whatever value it might have.<sup>4</sup> The data for Fig. 2 are listed in tabular form in Table 1 and data for Fig. 3 are shown in Table 2.

Equation (2) closely approximates the data points plotted in Fig. 2. These points are all for a 45° station, the approximate location of the maximum piezometric head differential and the smallest magnitude of  $h_1$ . Thus,  $h_1$  (min.) has been shown to be closely associated with potential flow piezometric head distribution, through the use of Equation (2). To be shown, is the numerical relation of Equation (2) to the magnitude of  $h_1$  (min.).

#### Measurement of "Mean" Piezometric Head

To reiterate, in potential flow,  $vn = a$  constant, then the constant,  $K$ , can be expressed as:  $K = v_1 r_1 = v_0 r_0 = V r_m$ ; where  $V$  is the average velocity. Therefore, in terms of Equations (1) and (2),

$$r_m = \frac{K}{V} = \frac{2c}{\ln r_0/r_1} = \frac{2c}{\ln \left( \frac{x+1}{x-1} \right)} = \frac{c}{2} (x^2-1) \sqrt{\frac{C_k}{x}} \quad . \quad . \quad (3)$$

As previously mentioned,  $r_m$  is the theoretical radius at which the tangential velocity is equal to the average velocity in the approach conduit. This radius is less than the centerline radius and is a function of the bend geometry.<sup>5</sup>

In the case of the Waynesboro bend, the mean radius  $r_m = 0.968 R$  and for Lell  $r_m = 0.911 R$ ; therefore, the use of centerline taps at  $R$  to measure the "mean" piezometric head ( $h_m$ ) for these given cross-sections should not introduce a grievous error. For convenience and other reasons to be shown later, the use of taps along the centerline is advantageous. (In a model study, limitations of time and funds may restrict the number of points of measurement).

#### The Energy in the Bend

In order to compare the piezometric head at  $r_m$  with that at the centerline,  $R$ , Fig. 4 has been prepared from one of Lell's experiments (interpolated from his data for both radii with good accuracy). Figure 5 has been plotted using Waynesboro data; however, piezometer taps were located only along the

4. From his plots in Fig. 34, page 34 and Diagram 52, page 61 where

$$C_k = \frac{\Delta p_{wa}}{q} + \frac{\Delta p_{wi}}{q} + S_{kr}$$

(Claims data not consistent for  $x$  less than 3.0).

5.  $r_m$  has no significance except at the cross-section where the maximum  $(h_0 - h_1)$  occurs, since  $r_m$  must approach  $R$  in magnitude towards the entrance and exit tangents of the bend.

centerline of each of the four sides. (In Fig. 4, the " $r_m$ " radius was applied from P.C. to P.T. for comparison.)

Note that there appears to be a restoration of energy prior to the mid-section of the bends, which is quite typical. The calculated, potential flow values of maximum and minimum velocity heads have been added to the figures at  $45^\circ$ , plotted from the total energy represented by the sum of the average velocity head and the centerline piezometric head. A very close balance in values is obtained for both  $h_1(\text{min.})$  and  $h_0(\text{max.})$ . Somewhat surprising is the fact that plotting from the "mean" energy line at  $r_m$  would yield a greater difference, or error, in Fig. 4.

The usual approach in drawing a piezometric head line for a bend is to draw a straight line between the P.C. and P.T., the slope being fixed by the bend loss assumed. It appears that such a procedure would result in a large error in some cases. Unfortunately there is no way to predict the value of the centerline piezometric head, except on an empirical basis.

#### Physical Applications

By the following method, a designer may predict with reasonable certainty whether cavitation might occur in a selected bend. First, the slope of the piezometric head line for the entrance and exit conduits should be determined, and the total energy line plotted  $V^2/2g$  above it. Extend the energy line of the entrance conduit to the  $45^\circ$  position of the bend, and connect it with the backward extension of the energy line of the exit conduit at the P.T. of the bend. This process is illustrated on Figs. 4 and 5 (broken line), and as can be seen, closely approximates the average total energy. The value of  $K$  can be conveniently determined from Equation (3). From the value of  $K$ ,  $v_1$  and  $v_0$  can also be calculated. By plotting distances equal to  $v_1^2/2g$  and  $v_0^2/2g$  below the synthetic total energy line, as shown in Figs. 4 and 5, approximate values of piezometric head (maximum on the outside and minimum on the inside) for the inner and outer radii of the bend can be found.

This approach should be useful in correlating the piezometric heads observed in model tests to those which can be expected in the prototype, particularly since it is convenient and customary to use taps located at the radius  $R$ . Correlation should be good for higher values of the ratio  $r_m/R$ . Unfortunately, there is no known complete data available for values of  $r_m/R$  less than the 0.911 used by Lell.

In many instances, probable low pressures can be safely avoided by utilizing sufficiently large radii of curvature.

The effect of velocity distribution upstream from a given rectangular bend, the effect of bend losses and a more limited presentation of pressure distribution in circular bends may be found in Reference (1).

It is interesting to note in passing that the station at which the maximum ( $h_0 = h_1$ ) occurs with circular bends appears to be at  $22.5^\circ$ , for  $45^\circ$ ,  $90^\circ$  and  $180^\circ$  bends.<sup>(12)</sup> This observation has recently been reasonably verified for  $90^\circ$  circular bends;<sup>(2)</sup> correlation with potential flow was also obtained.

In the light of the experience with circular bends, together with the observation of near-potential flow in model studies with  $45^\circ$  to  $135^\circ$  rectangular bends by several experimenters, the utilization of the techniques presented here can probably be applied with good accuracy to bends of  $45^\circ$  to  $180^\circ$ .

The data from which Table 1 was obtained include a wide range of velocities. There was no evidence noted of any viscous effects for any of the data. Reynolds numbers for prototype structures would normally be larger.

### Cavitation Tests

Apparently the vapor pressure has not been reached in reported model tests on bends. The foregoing presentation can be adapted to anticipatory evaluation of critical cavitation conditions. "A useful index for the cavitation phenomenon is . . . called the cavitation number."<sup>(15)</sup>

$$\sigma = \frac{h-h_v}{V^2/2g}$$

in which  $h$  is the piezometric head at an upstream station in uniform flow (or,  $h_m$  could possibly be used),  $h_v$  is the minimum piezometric head including the vapor pressure and  $V$  is the average velocity at the reference station where  $h$  is measured.

For irrotational flow,

$$\sigma = \left( \frac{v_1}{V} \right)^2 - 1$$

and from Equation (3),

$$\frac{K}{V} = \frac{v_1 r_1}{V} = \frac{v_1}{V} c(x-1) = \frac{c}{2} (x^2-1) \sqrt{\frac{C_k}{x}}$$

from which

$$\sigma = \frac{C_k}{4x} (x+1)^2 - 1$$

or,

$$\sigma = \frac{4}{(x-1)^2 \left( 1 + \frac{x+1}{x-1} \right)^2} - 1 \quad . \quad . \quad . \quad (4)$$

Combinations of  $V$  and  $h$  which will provide theoretical cavitation conditions can easily be computed from the above, but no allowance has been made for a loss term between the reference station and the inside of the bend. The following table has been made using Equation (4):

$x$	$\sigma$
2	2.32
3	1.08
4	0.70
5	0.52

### SUMMARY AND CONCLUSIONS

The results obtained in this study lead to the following conclusions with regard to hydraulic bends of rectangular cross-section:

- 1) Measured pressures are closely related to potential flow piezometric head distribution.
- 2) The maximum differential piezometric head across the bend can be

expressed in terms of potential flow relationships and the geometry of the bend.

3. The point of minimum piezometric head is associated with the location of the maximum differential piezometric head, occurring at about  $45^\circ$  for  $90^\circ$  and  $180^\circ$  bends. This should be true for any angle between  $90^\circ$  and  $180^\circ$  and probably applies to angles slightly less than  $90^\circ$ .
4. The total energy at the  $45^\circ$  station for  $90^\circ$  and  $180^\circ$  bends with  $r_m/R > 0.9$  apparently is found at the radius  $R$  and not  $r_m$ , using the kinetic energy represented by the average velocity of the flow section.
5. A technique for predicting the mean piezometric head at the  $45^\circ$  station has been advanced. Using this head, the probable minimum piezometric head can be computed.
6. The material presented can be advantageously employed in determining a sufficiently large radius of curvature to avoid cavitation. The evidence submitted should be of value in analyzing the results of model tests, provided that piezometric head measurements at the mid-height of the inside and outside walls are included, particularly in the vicinity of the  $45^\circ$  cross-section of the bend.
7. No viscous effects were noted in any of the data studied. The effect of viscosity would be even less in full-scale dam outlets, siphons or outlet conduit bends.

#### REFERENCES

1. McPherson, M.B., "The Design of Bends for Hydraulic Structures," unpublished professional degree thesis, Bucknell University Library, April 20, 1952.
2. Taylor, D.C. and McPherson, M.B., "Elbow Meter Performance," Journal of the American Water Works Association, November, 1954.
3. Pfarr, Die Turbinen für Wasserkraftbetrieb, 2nd Edition, pp. 36, Berlin 1912.
4. Lell, J., "Beitrag zur Kenntnis Der Sekundärströmungen in Gekrümmten Kanälen," Dissertation, R. Oldenbourg, München, 1913.
5. Shukry, A., Discussion of "Determination of Pressures Within a Siphon Spillway," by I.M. Nelidov, A.S.C.E. Trans., 1946.
6. Davies and Puranik, "The Flow of Water Through Rectangular Pipe Bends," Journal Institute of Civil Engineers, London, Vol. 2, 1935-36.
7. Gibson, Asprey and Tattersall, "Model Tests on Siphon Spillways," Minutes of Proceedings, Institute of Civil Engineers, London, Vol. 231, 1931.
8. Yarnell, D.L. and Woodward, S.M., "Flow of Water Around 180-Degree Bends," U.S. Department of Agriculture, Technical Bulletin No. 526, 1936.
9. Silberman, E., "The Nature of Flow in an Elbow," Project Report No. 5, St. Anthony Falls Hydraulic Laboratory, University of Minnesota, 1947.
10. Lansford, W.M., "The Use of an Elbow in a Pipe Line for Determining the Rate of Flow in the Pipe," University of Illinois Engineering Experiment Station, Bulletin No. 289, December, 1936.
11. Nippert, H. "Über den Strömungsverlust in Gekrümmten Kanälen," V.D.I., Forschungsarbeiten, Heft 320, Berlin, 1929.

12. Yarnell, D.L., "Flow of Water Through 6-Inch Pipe Bends," U.S. Department of Agriculture, Technical Bulletin No. 577, 1937.
13. Wattendorf, F.L., "A Study of the Effect of Curvature on Fully Developed Turbulent Flow," Proceedings of the Royal Society of London, Series A, Vol. 148, pp. 565-598, February, 1935.
14. Addison, H., "The Use of Bends as Flow Meters," Engineering, pp. 227-229, March 4, 1938.
15. Rouse, H., Engineering Hydraulics, pp. 29-31, John Wiley & Sons, 1950.

Table 1

Rectangular Bends - General

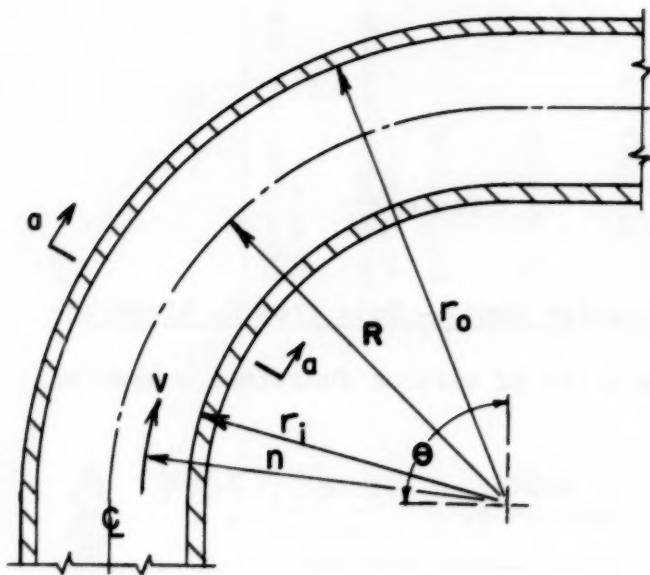
Source of Data	Bend Radius, R	Half- Thickness, c	Width b	R/c = x	Angle of Bend, $\theta$	C <sub>k</sub> at 45°	C <sub>k</sub> at 90°	Remarks
Addison (14)	11.00 cm 11.87 12.19	2.99 cm 2.99 3.00	6.00 cm 6.00 6.00	3.68 3.97 4.06	90° 90° 90°	1.18 1.11 1.06		Calculated; average of data
Silberman (Water)	12 in	3 in	6 in	4.0	90°	1.12		Calculated; average of 5 runs
Waynesboro 1:20 Model	6.75 in	2.10 in	4.20 in	3.21	90°	1.415		Calibration
Mt. Alto 1:16 Model	8.81 in	2.44 in	4.88 in	3.62	90°	1.25		Calibration
Yarnell & Woodward	10 in 7.5 12.5	5 in 2.5 2.5	10 in 10 10	2.0 3.0 5.0	180° 180° 180°	~3.2 ~1.65 ~0.96	~2.68 ~1.53 ~0.92	By scaling; two rates of flow, only
Lell	20 cm	10 cm	10 cm	2.00	180°	2.90	2.61	Data for 12 runs; averaged at 3, 6 and 9 m./sec.
Wattendorf (13)	22.5 cm	2.5 cm	90 cm	9.0	300°	(2.83 @ 56.25°)	0.53	By scaling; 3 runs only. Same value 300 to 2400

Table 2

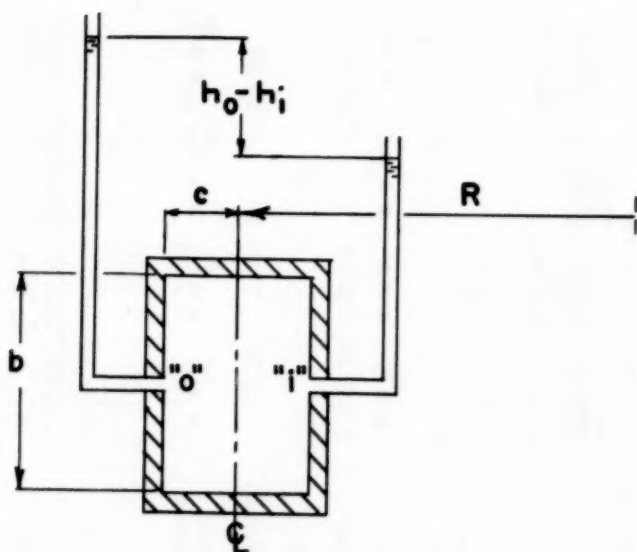
90° Rectangular Bends - Data from H. Nippert

(By scaling plots of various functions presented)

Bend Radius, R	Half- thickness, c	Width b	R/c = x	C <sub>k</sub> at 45°
22.5 mm	7.5 mm	60 mm	3.00	1.74
32.5	"	"	4.34	1.13
45.0	"	"	6.00	0.80
57.5	"	"	7.66	0.55
25.0	12.5	60	2.0	2.60
37.5	"	"	3.0	1.68
62.5	"	"	5.0	0.85
60	30	25	2.0	1.99
90	"	"	3.0	1.51
150	"	"	5.0	0.85
210	"	"	7.0	0.55
11.2	4	60	2.8	1.76
23.2	"	"	5.8	0.75
36.0	"	"	9.0	0.53
60	30	15	2.0	2.10
90	"	"	3.0	1.41
150	"	"	5.0	0.93



TYPICAL BEND SECTION



Section a-a

Figure 1.

# RECTANGULAR BENDS

$C_k$  vs.  $x$

for  $(h_o - h_i)$  at  $45^\circ$

ADDISON - $90^\circ$	○
YARNELL - $180^\circ$	▽
WAYNESBORO - $90^\circ$	⊗
MT. ALTO - $90^\circ$	⊕
LELL - $180^\circ$	▽
SILBERMAN - $90^\circ$	△
WATTENDORF - $300^\circ$	▲

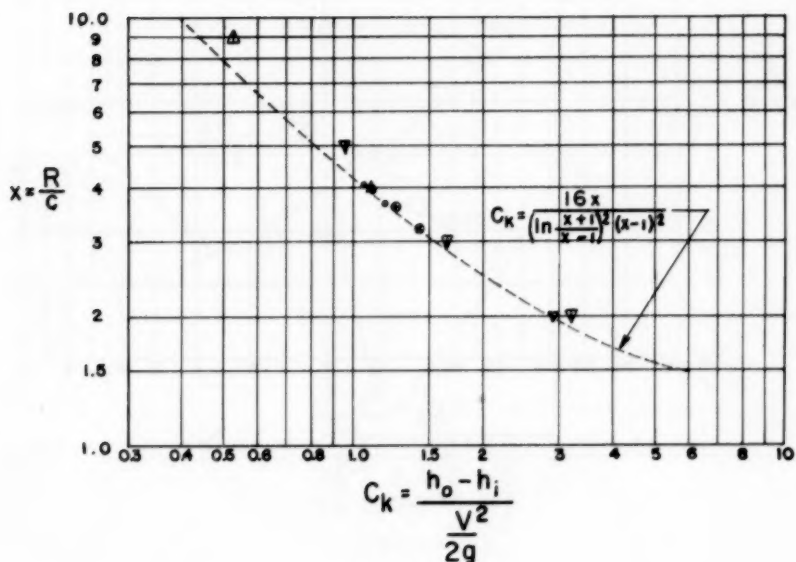


Figure 2.

# RECTANGULAR BENDS

$C_k$  vs.  $x$   
from H. Nippert-90°  
for  $(h_o-h_i)$  at 45°

$b \times 2c$  (mm.)

60 x 15	⊙
60 x 25	⊕
60 x 8	⊗
25 x 60	△
15 x 60	▲

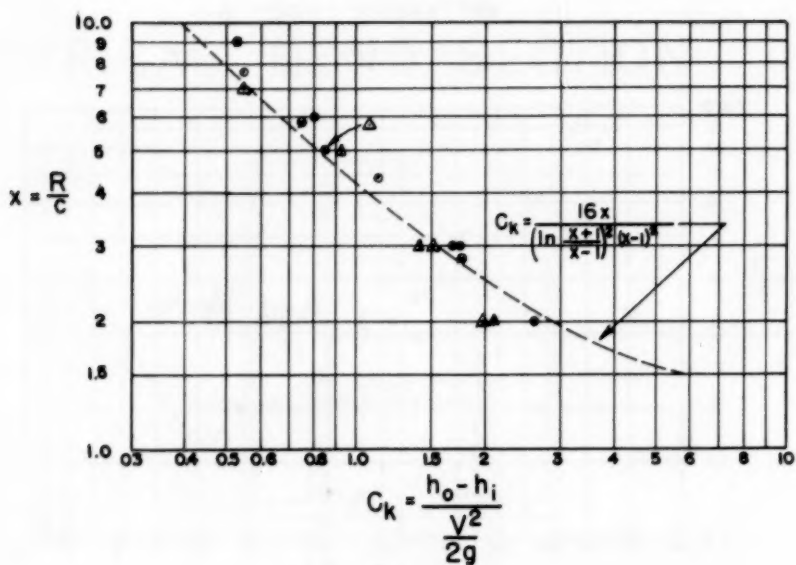


Figure 3.

# RECTANGULAR BEND by LELL

$\theta = 180^\circ$

from typical data for  $V = 9$  m./sec.

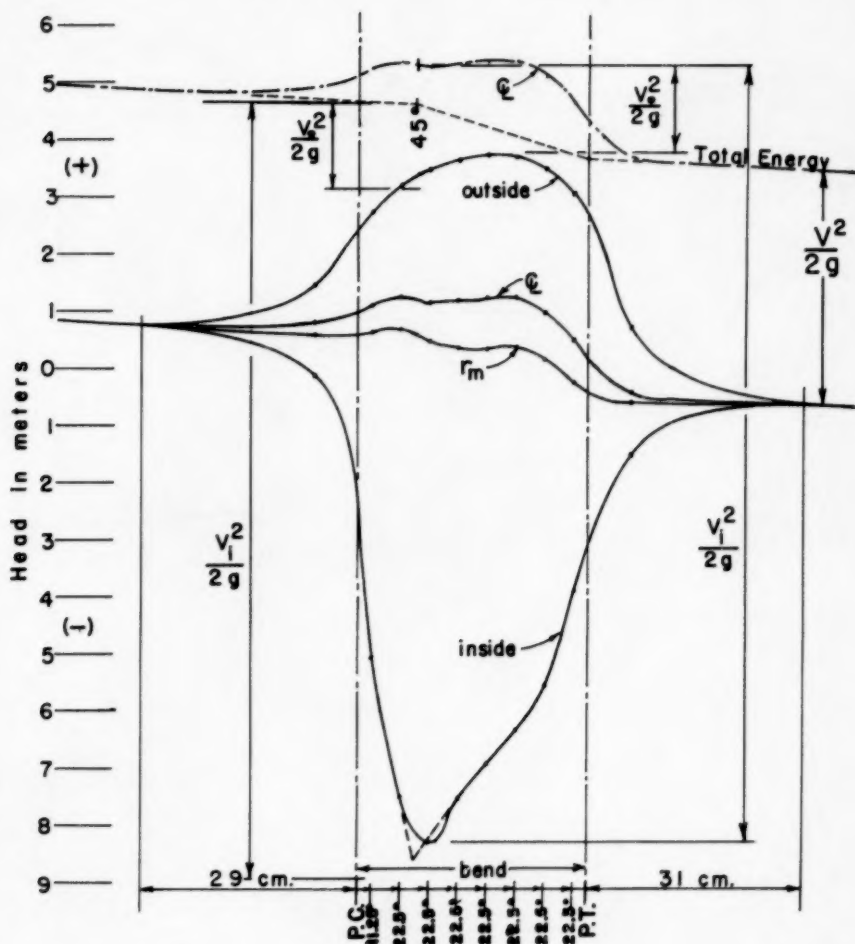


Figure 4.

# RECTANGULAR BEND - WAYNESBORO

$\theta = 90^\circ$

Test D-I-D,  $V = 9.93$  ft./sec.

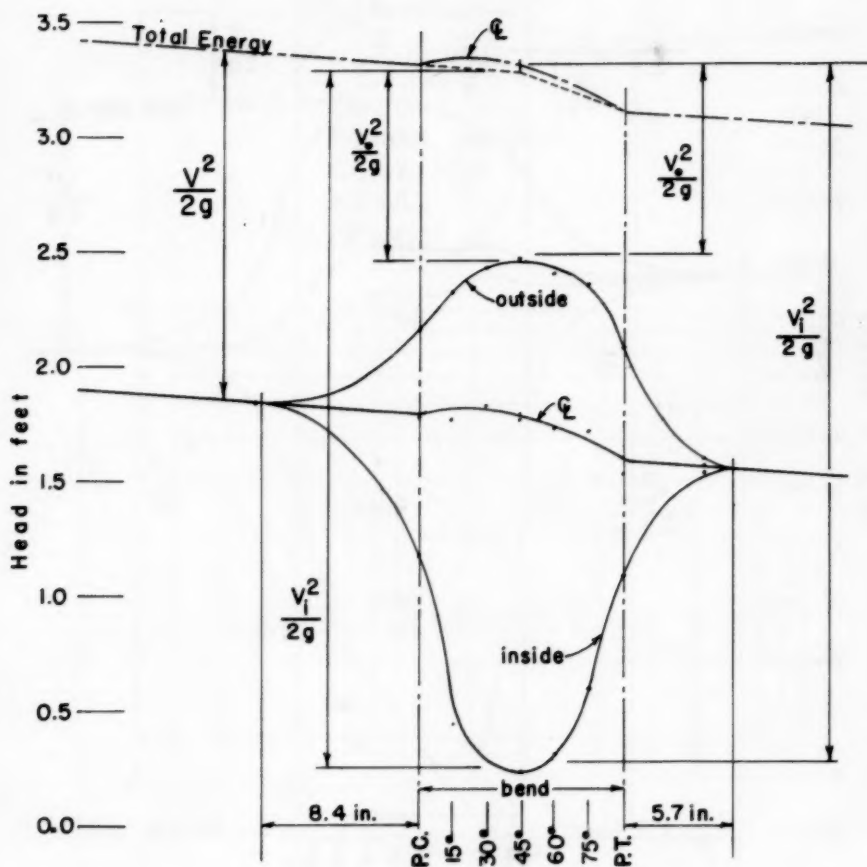


Figure 5.